1987

NASA/ASEE SUMMER FACULTY RESEARCH FELLOWSHIP PROGRAM

MARSHALL SPACE FLIGHT CENTER
THE UNIVERSITY OF ALABAMA IN HUNTSVILLE

THE JEFFCOTT EQUATIONS IN NONLINEAR ROTORDYNAMICS

Prepared By:	R. A. Zalik
Academic Rank:	Professor
University and Department:	Auburn University Algebra, Combinatorics, and Analysis

NASA/MSFC:

Laboratory:	Structures and Dynamics
Division:	Control Systems
Branch:	Mechanical Systems

| NASA Colleague: | Tom Fox |

The Jeffcott Equations in Nonlinear Rotordynamics

R. A. Zalik

Auburn University

Division of Mathematics

120 Mathematics Annex Building

Auburn, AL   36849-3509

Acknowledgement

Abstract. The Jeffcott equations are a system of coupled differential

equations that represent the behavior of a rotating shaft. This is a simple

model that allows investigation of the basic dynamic behavior of rotating

machinery. Nonlinearities can be introduced by taking into consideration

deadband, side force, and rubbing, among others.

In this paper we study the properties of the solutions of the Jeffcott

equations with deadband. In particular, we show how bounds for the solutions

of these equations can be obtained from bounds for the solutions of the

linearized equations. By studying the behavior of the Fourier transforms of

the solutions, we are also able to predict the onset of destructive

vibrations. These conclusions are verified by means of numerical solutions

of the equations, and of power spectrum density (PSD) plots.

This study offers insight into a possible detection method to determine

pump stability margins during flight and hot fire tests, and was motivated by

the need to explain a phenomenon observed in the development phase of the

cryogenic pumps of the Space Shuttle, during hot fire ground testing: namely,

the appearance of vibrations at frequencies that could not be accounted for

by means of linear models.

1. Introduction

H. H. Jeffcott [10] was one of the first to study the vibration characteristics of an unbalanced, uniform, flexible shaft supported by bearings. He did so by considering a linear system of differential equations of the form

$$y'' + Cy' + Ay = F \cos wt$$

$$z'' + Cz' + Az = F \sin wt \tag{1}$$

where the differentiation is with respect to the parameter t, and the shaft is assumed to rotate along the x-axis with angular velocity w, y and z describe the displacement of the center of the shaft, and the coefficients have the following physical interpretation: $C = C_s/m$, $A = K_s/m$, $K = K_b/m$, and $F = uw^2$, whre m is the mass of the shaft, C_s is the seal damping, K_s and K_b are the seal and bearing stiffnesses, and u is the displacement of the shaft's center of mass from the geometric center.

In [12] Yamamoto studied the effect of deadband (i.e. the clearing between housing and bearing), but his treatment was not rigorous. Other works dealing with nonlinearities include [3], [4], [8] and [11]. In [7], Day used the method of multiple scales to gain new insight into the properties of the solutions. He discovered a frequency, which he termed "nonlinear natural frequency" that appears in the PSD plots of solutions of the nonlinear model and is absent from the PSD plots of solutions of the linear model. The nonlinear natural frequency seems to have been observed during early ground testing of both LOX and fuel pumps of the second stage Main Engine of the Space Shuttle but, until now, there has been no explanation of its origin.

If $r = (y^2 + z^2)^{1/2}$, δ is the deadband, $K = K_b/m$, where K_b is the bearing stiffness, $B = Q_s/m$, with Q_s denoting the cross-coupling stiffness of the seal, and

$$h(t) = \begin{cases} 1 & \text{if } r < \delta \\ \\ \delta/r & \text{if } r > \delta, \end{cases} \tag{2}$$

then the model studied by Day can be described by the system

$$y'' + Cy' + [A + K(1-h)]y + Bz = f_1(t), \tag{3}$$

$$z'' + Cz' - By + [A + K(1-h)]z = f_2(t),$$

where $f_1(t) = F \cos wt$, $f_2(t) = F \sin wt$, and $K(1-h)$ is the nonlinearity associated with the deadband (see Fig. 1). Note that (1) is a particular case of (3).

In this paper we shall explain the nature of the nonlinear natural frequency and apply our conclusions to the signature analysis of the nonlinear Jeffcott model described by (3), where $f_1(t)$ and $f_2(t)$ are arbitrary bounded and continuous functions, B, C, K, and δ are positive, and A and t are nonnegative.

2. Properties of the solutions of Jeffcott's equations.

2.1 Existence, uniqueness, and a representation formula.

If $x_1 = y$, $x_2 = y'$, $x_3 = z$, $x_4 = z'$, $r = (x_1^2 + x_3^2)^{1/2}$ and $h(t)$ is given by (2), then (3) is equivalent to

$$x_1' = x_2$$

$$x_2' = - [A + K(1-h)]x_1 - Cx_2 - Bx_3 + f_1(t) \qquad (4)$$

$$x_3' = x_4$$

$$x_4' = - Bx_1 - [A + K(1-n)]x_3 - Cx_4 + f_2(t)$$

or, more concisely,

$$\underline{x}' = \underline{g}(\underline{x},t).$$

Since $\underline{g}(\underline{x},t)$ is continuous, and satisfies a Lipschitz condition on $\underline{x}$, from

standard existence and uniqueness theorems (cf., eg. [5]), we know that

every initial value problem for (4) has a unique solution. Thus, we also

infer that every initial value problem for (3) has a unique solution. Let

$v = y + iz$, $f(t) = f_1(t) + if_2(t)$, and $M = A + K - iB$; then (3) is also

equivalent to

$$v'' + Cv' + Mv - Khv = f(t). \qquad (5)$$

Before studying (5), let us first consider a linear system of the form

$$v'' + Cv' + Mv = g(t). \qquad (6)$$

Then

$$v = C_1 \exp(\lambda_1 t) + C_2 \exp(\lambda_2 t) + v_p, \text{ where } C_1 \exp(\lambda, t) + C_2 \exp(\lambda_2 t) \text{ is a}$$

solution of

$$v'' + Cv' + Mv = 0, \tag{7}$$

and therefore $\lambda_{1,2} = (1/2) [- C \pm (C^2 - 4M)^{1/2}]$. If $Q = C^2 - 4(A + K)$, a

straightforward computation shows that $\lambda_1 = \alpha + i\beta$, $\lambda_2 = \alpha' - i\beta$, where

$$\beta = 8^{-1/2} [-Q + (Q^2 + 16 B^2)^{1/2}]^{1/2}, \tag{8}$$

$$\alpha = [\beta^{-1} B - C]/2 \qquad , \quad \alpha' = -[\beta^{-1} B + C]/2, \tag{9}$$

and therefore

$$\alpha' = -\beta^{-1} B + \alpha \tag{10}$$

Applying, e.g. [5, Theorem 6.4] we readily deduce that the Green's function

of the differential operator $(d^2/dt^2) + C(d/dt) + M$ is $G(t - s)$, where

$$G(t) = (\lambda_2 - \lambda_1)^{-1} [\exp(\lambda_1 t) + \exp(\lambda_2 t)], \text{ i.e. } \int_0^t G(t-s)q(s)ds \text{ is a}$$

particular solution of (6), and therefore

$$v = c_1 \exp(\lambda_1 t) + c_2 \exp(\lambda_2 t) + \int_0^t G(t-s)q(s)ds.$$

If in particular $g(s) = K\, h(s)\, v(s) + f(s)$, then (6) reduces to (5), and we have:

$$v = c_1 \exp(\lambda_1 t) + c_2 \exp(\lambda_2 t) + \int_0^t G(t-s)f(s)ds + K\int_0^t G((t-s)h(s)v(s)ds.$$

In other words,

$$v(t) = u(t) + P(t), \tag{11}$$

where

$$u(t) = c_1 \exp(\lambda_1 t) + c_2 \exp(\lambda_2 t) + \int_0^t G(t-s)f(s)ds \tag{12}$$

is a solution of the linear differential equation $v'' + Cv' + Mv = f(t)$,

(henceforth called the <u>linear part</u> of (5)), and

$$P(t) = K\int_0^t G(t-s)\, h(s)v(s)ds. \tag{13}$$

Note that we have a closed form formula for u, whereas $P(t)$ is expressed in terms of the unknown function $v(t)$. Our analyses will be based on a study of the properties of the perturbation term $P(t)$.

2.2 Bounds.

The definition (2) of $h(s)$ implies that $\left|h(t)v(t)\right| \leq \delta$; thus,

$$\left|P(t)\right| \leq K\delta \int_0^t \left|G(t-s)\right| ds \leq$$

$$K\delta \, (\beta^{-2} B^2 + 4 \beta^2)^{-1/2} \int_0^t [\exp\,(\alpha(t-s)) + \exp(\alpha'(t-s))] ds.$$

Since (9) and (10) imply that if $\alpha = 0$, then $\beta = B/C$, and when $\alpha = \beta^{-1}B$

then $\alpha' = 0$, we have

$$\left|P(t)\right| \leq \begin{cases} K\delta(\beta^{-2}B^2 + 4\beta^2)^{-1/2}[(1/\alpha)(\exp(\alpha t)-1) + (1/\alpha')(\exp(\alpha't)-1)] \\ \qquad\qquad\qquad\qquad\qquad \text{if } \alpha \neq 0, \beta^{-1}B \\[2mm] K\delta(C^2 + 4B^2/C^2)^{1/2}[t + (2/C)(1-\exp[(-C/2)t])) \\ \qquad\qquad\qquad\qquad\qquad \text{if } \alpha = 0, \\[2mm] K\delta(\beta^{-2}B^2 + 4\beta^2)^{-1/2}[(\beta/B)(\exp[(B/\beta)t] -1) + t] \\ \qquad\qquad\qquad\qquad\qquad \text{if } \alpha = \beta^{-1}B \end{cases} \qquad (14)$$

From (11), (12), (13), and (14) we derive the following conclusions:

1. If $\alpha < 0$ and $\left|\int_0^t G(t-s) \, f(s)ds\right| \leq M$, then the steady state

solution v_∞ of (5) satisfies the following inequality:

$$\left|v_\infty\right| \leq M + K\delta(\beta^{-2}B^2 + 4\beta^2)^{-1/2}\left|1/\alpha + 1/\alpha'\right|$$

2. If $\alpha = 0$, the perturbation term $P(t)$ can grow at most linearly.

3. If $\alpha > 0$, the order of growth of $P(t)$ cannot exceed $\exp(\alpha t)$; note that the order of magnitude of all nonzero solutions of (7) cannot exceed $\exp(\alpha t)$.

Thus, since we have assumed that $f(t)$ is bounded, the study of the boundedness of the solutions of (5) reduces to the study of the boundedness of the solutions of its homogeneous part. If $\alpha < 0$ we shall say that (5) is stable, if $\alpha > 0$ that (5) is unstable, and if $\alpha = 0$ that (5) has reached the stability boundary. This nomenclature is consistent with that used for linear systems (cf. [9, pp. 83, 84]).

2.3 Estimates for β.

In this section we will prove that β is between B/C and $(A+K)^{1/2}$. The importance of this observation will become clear in the sequel. In what follows, let $\gamma = A + K$ and $\xi = (B/C)^2$; thus $Q = C^2 - 4\gamma$.

Assume that $\alpha < 0$; then from (9) we see that $B/C < \beta$. Squaring and applying (8), we have

$$\xi < (1/8) \; [- Q + (Q^2 + 16 \; B^2)^{1/2}].$$

Thus, ξ satisfies the inequality $4\xi^2 + Q\xi - B^2 < 0$, which can be written as

$4\xi^2 + [C^2 - 4\gamma] \; \xi - B^2 < 0$, or

$C^2 - 4\gamma < (B^2 - 4\xi^2) \; \xi^{-1} = B^2\xi^{-1} - 4\xi$. Since $\xi = (B/C)^2$, we have that

$C^2 - 4\gamma < C^2 - 4\xi$, and therefore $\gamma > \xi$, i.e.

$$B^2 < C^2\gamma$$

Thus,

$$16\gamma^2 + C^4 - 8C^2\gamma + 16B^2 < 16\gamma^2 + C^4 + 8C^2\gamma,$$

i.e.

$$Q^2 + 16B^2 < (4\gamma + C^2)^2,$$

and therefore

$$[Q^2 + 16 \; B^2]^{1/2} < 4\gamma + C^2.$$

Subtracting Q from both sides of this inequality we see that

$$8\beta^2 = - Q + [Q^2 + 16B^2]^{1/2} < 8\gamma,$$

and we conclude that $\beta < (A + K)^{1/2}$.

The cases $\alpha = 0$ and $\alpha > 0$ are treated similarly, and we shall omit the details. The conclusions are the following:

1. If $\alpha < 0$, then $B/C < \beta < (A + K)^{1/2}$, and $\alpha' < 0$.

2. If $\alpha = 0$, then $B/C = \beta = (A + K)^{1/2}$, and $\alpha' < 0$.

3. If $\alpha > 0$, then $(A + K)^{1/2} < \beta < B/C$.

From these conclusions we also infer that if $f(t)$ is bounded, then (5) is stable if and only if $B/C < (A + K)^{1/2}$.

2.4 Resonance.

From the results of 2.3 it is clear that (5) is in resonance if and only if its linear part is in resonance. If for example $f(t) = F_0 \exp(iwt)$, then we

readily see that the linear part of (5) has a particular solution of the form $A_0 \exp(iwt)$, where

$$A_0 = F_0 / [(A + K - W^2) + i(w-\beta)].$$

Since the denominator in the preceding formula vanishes if and only if $\beta = w$ and $w = (A + K)^{1/2}$, we deduce that $\beta = (A + K)^{1/2}$, and therefore that $\alpha = 0$. Thus (5) can be in resonance only on the stability boundary.

3. Harmonic Analysis of the solutions.

3.1 Introduction

In practice, the coefficients of (5) and, in general, the equations that describe the movement of rotating machinery, are imperfectly known. The approach taken is to sample the system response over a time interval (in our case, that would mean measuring $y(t_i)$ and $z(t_i)$, $i = 0, \ldots, N$, where the t_i are equally spaced points), and to approximate the Fourier transforms of

y(t) and z(t) by means of the Discrete Fourier Transforms of the sequences

$\{y(t_i)\}$ and $\{z(t_i)\}$. (See, e.g. [1]). The absolute values of the

coefficients in the Discrete Fourier expansions are then plotted on graphs

called Power Spectrum Density (PSD) plots, which represent the response of

the mechanical system at different frequencies. One then tries to determine

the condition of the mechanical system by an examination of these plots.

This is known as "signature analysis". (See, e.g. Collacott [6].) In this

section we examine the properties of the Fourier transforms of the solutions

of (5), whereas in section 4 we show, by means of examples, how to apply

these conclusions to the signature analysis of the system.

From now on, we shall assume that $\alpha < 0$.

3.2 Properties of the continuous Fourier transform.

Let G(t), v(t), u(t), and P(t) be defined to equal 0 for $t < 0$. Then

(11) is valid on $(-\infty, \infty)$. If

$$q(t) = h(t) \, v(t),$$

it is clear that $q(t)$ vanishes for $t < 0$. Thus, from (13) we readily see that

$$P(t) = K\int_{-\infty}^{\infty} G(t-x) \, q(x)dx = K(G * q)(t), \qquad (15)$$

where "*" denotes the convolution product. If $p_1(t) = \exp(\lambda_1 t)$,

$p_2(t) = \exp(\lambda_2 t)$ for $t \geq 0$, and equal zero for $t < 0$, and $u_p(t)$ denotes

a particular solution of the linear part of (5), then (11) can be written in

the form

$$v(t) = c_1 \, p_1(t) + c_2 \, p_2(t) + u_p(t) + P(t). \qquad (16)$$

Note, moreover, that

$$G(t) = (\lambda_2 - \lambda_1)^{-1}[p_1(t) + p_2(t)] \quad \text{and therefore}$$

$$P(t) = (\lambda_2 - \lambda_1)^{-1} \, [(p_1 + p_2) * q] \, (t). \qquad (17)$$

Let F denote the Fourier transform operator; thus, if $g(t)$ is

integrable on $(-\infty, \infty)$, then $F[g](s) = \int_{-\infty}^{\infty} g(t) \exp(-ist)dt$.

In particular, when $\alpha < 0$ we have

$$F[p_1](s) = 1/[i(s - \beta) - \alpha] \qquad (18)$$

and

$$F[p_2](s) = 1/[i(s + \beta) - \alpha + \beta^{-1}B]. \qquad (19)$$

If $u_p(t)$ and $q(t)$ are integrable on $(-\infty, \infty)$, from (16) and (17) we

see that

$$F[v] = c_1 F[p_1] + c_2 F[p_2] + F[u_p] + (\lambda_2 - \lambda_1)^{-1}(F[p_1] + F[p_2]) F(q).$$

Since $F[p_1](\beta)$ diverges as $\alpha \to 0^-$, we therefore conclude that if α

approaches 0 from the left, then the graphs of the real and imaginary parts

of $F[v]$ will exhibit increasingly large spikes at β, where α and β are

linked by (9). At first glance, this does not appear to be very useful,

since in most applications u_p will not be integrable on $(-\infty, \infty)$ (as for

example when $f(t) = F \exp(iwt))$. We shall now show that the range of

validity of our conclusions can be greatly extended if we consider windows.

3.3 Windowing and the nonlinear natural frequency

3.3.1 Analysis of the transient terms

In practice, Fourier transforms are computed for samples taken over a time

interval of the form (a,b), (called a "window"), where a is in general

larger than zero. Let $g^{(a,b)}(t) = g(t)$ if $a \leq t \leq b$, let $g^{(a,b)}(t)$

equal zero otherwise, and let $g^{(b)} = g^{(0,b)}$. Clearly

$$F[p_1^{(a,b)}](s) = [\exp(\lambda_1 - si)b - \exp(\lambda_1 - si)a]/(\lambda_1 - si),$$

and

$$F[p_2^{(a,b)}](s) = [\exp(\lambda_2 - si)b - \exp(\lambda_2 - si)a]/(\lambda_2 - si).$$

Since $\lambda_1 - \beta i = \alpha$, we see that $F[p_1^{(a,b)}](\beta)$ diverges as $\alpha \rightarrow 0^-$; thus,

also the graphs of the real and imaginary parts of $F[v^{(a,b)}]$ should have

spikes at β. However, since $\lim\limits_{a \rightarrow \infty} F[p_1^{(a,b)}](s) = \lim\limits_{a \rightarrow \infty} F[p_1^{(a,b)}](s) = 0$, we

conclude that for fixed α and sufficiently large a, these spikes may be

detected only if α is extremely close to 0. (Whether they will be

detected at all depends on the numerical stability of the computations).

Thus, in order to obtain useful data we have to analyze the Fourier transform

of the perturbation term $P(t)$.

3.3.2 Analysis of the perturbation term

Let $P_b(t) = K \int_{-\infty}^{\infty} G(t-x) \, q^{(b)}(x) \, dx = \int_0^t G(t - x) \, q^{(b)}(x) \, dx$. From (15) we

see that if $t \leq b$, then $P_b(t) = P(t)$, whereas for $t \geq b$,

$P_b(t) = \int_0^b G(t - x) \, q(x) \, dx$. Thus,

$$F[P^{(b)}](s) = F[P_b](s) - K \, I_b(s), \qquad (20)$$

where

$$I_b(s) = \int_b^{\infty} \exp(-st1) \int_0^b G(t - x) \, q(x) \, dx \, dt.$$

We can write I_b in the form

$$I_b = (\lambda_2 - \lambda_1)^{-1} \, [I(\lambda_1) - I(\lambda_2)],$$

with

$I(\lambda) = \int_b^\infty \exp(-sti) \int_0^b \exp[\lambda(t - x)] \, q(x) \, dx \, dt.$

If $\text{Re}(\lambda) < 0$, reversing the order of integration we have:

$I(\lambda) = \int_0^b \exp(-\lambda x) q(x) dx \int_b^\infty \exp[(\lambda - si)] dt$

$$= M(b, \lambda) \exp[(\lambda - si)b]/(\lambda - si),$$

where $M(b, \lambda) = \int_0^b \exp(-\lambda x) q(x) \, dx.$

Thus,

$$I_b = (\lambda_2 - \lambda_1)^{-1} M(b, \lambda_1) \exp[(\lambda_1 - si)b]/(\lambda_1 - si)$$

$$\qquad (21)$$

$$+ (\lambda_2 - \lambda_1)^{-1} M(b, \lambda_2) \exp[\lambda_2 - si)b]/(\lambda_2 - si).$$

Moreover, since $q^{(b)}(x)$ is of bounded support it is integrable. Thus, since $P_b(t) = K (G * q_b)(t)$, we know that

$$F[P_b](s) = K \, F[G](s) \, F[q^{(b)}](s) \qquad (22)$$

Since $G(t) = (\lambda_2 - \lambda_1)^{-1} [p_1(t) + p_2(t)]$, from (18) and (19) we have:

$$F[G](s) = (\lambda_2 - \lambda_1)^{-1} [(\lambda_1 - si)^{-1} + (\lambda_2 - si)^{-1}].$$

Combining (20), (21), and (22), we thus obtain:

$$F[P^{(b)}](s) =$$

$$K(\lambda_2 - \lambda_1)^{-1} \{F[q^{(b)}](s) - M(b, \lambda_1)\exp[(\lambda_1 - si)b]\}/(\lambda_1 - si) +$$

$$K(\lambda_2 - \lambda_1)^{-1} \{F[q^{(b)}](s) - M(b, \lambda_2)\exp[(\lambda_2 - si)b]\}/(\lambda_2 - si).$$

Thus, since $F[P^{(a,b)}](s) = F[P^{(b)}](s) - F[P^{(a)}](s)$,

setting

$$Q(a, b, \lambda, s) = \tag{23}$$

$$F[q^{(a,b)}](s) - M(b, \lambda)\exp[(\lambda - si)b] + M(a, \lambda)\exp[(\lambda - si)a],$$

we conclude that

$$F[P^{(a,b)}](s) = Q(a, b, \lambda_1, s)/(\lambda_1 - si) + Q(a, b, \lambda_2, s)/(\lambda_2 - si). \tag{24}$$

If $Q(a, b, \lambda_1, \beta) \neq 0$, we conclude that $F[P^{(a,b)}](\beta)$ will diverge as

$\alpha \to 0^-$.

We shall now show that, for any $\varepsilon > 0$, the functions $Q(a, b, \lambda_1, s)$

and $Q(a, b, \lambda_2, s)$ are bounded, uniformly on s, provided that

$-\varepsilon < \alpha < 0$. From (23) it is clear that

$\left| Q(a,\ b,\ \lambda,\ s) \right| \leq \left| F[q^{(a,b)}](s) \right| + \left| M(b,\ \lambda) \right| + \left| M(a,\ \lambda) \right|$. Now, the

definition of $G(t)$ implies that $\left| G(t) \right| \leq 2 \left| \lambda_2 - \lambda_1 \right|^{-1}$. Since

$\left| h(t)v(t) \right| \leq \delta$, it is clear from (13) that $\left| P(t) \right| \leq 2K \left| \lambda_2 - \lambda_1 \right|^{-1} \delta t$.

Assuming that $\left| f(t) \right| \leq M_1$, it is readily seen from (11) and (12), that

$$\left| v(t) \right| \leq \left| C_1 \right| + \left| C_2 \right| + 2 \left| \lambda_2 - \lambda_1 \right|^{-1} (k\delta + M_1) t.$$

The constants C_1 and C_2 depend on the initial conditions. We shall now

show that, for the same set of initial conditions and any $\varepsilon > 0$, C_1 and C_2

are bounded, uniformly on α.

Assume that $v(0) = v_0$, and $v'(0) = v_1$. From (11), (12), and (13), it

is clear that

$$C_1 + C_2 = v_0. \tag{25}$$

On the other hand, since

$$(d/dt) \int_0^t G(t-x)g(x)dx = G(0)g(t) + \int_0^t (\partial/\partial t)G(t-x)g(x)dx,$$

(cf., e.g. Bartle [2]), differentiating (11) we have

$\lambda_1 c_1 + \lambda_2 c_2 + G(0)g(0) = v_1$, where $g(t) = f(t) + Kh(t)v(t)$, and from (25)

we obtain

$$\lambda_1 c_1 + \lambda_2(v_0 - c_1) + G(0)g(0) = v_1.$$

If $\left| f(t) \right| \leq M_1$, and $M = M_1 + K\delta v_0$, it is easy to see that $\left| g(0) \right| \leq M$.

Thus, since $G(0) = (\lambda_2 - \lambda_1)^{-1}$, we deduce that

$$\left| c_1 \right| \leq \left| \lambda_2 - \lambda_1 \right|^{-1} \left| \lambda_2 v_0 \right| + \left| \lambda_2 - \lambda_1 \right|^{-2} \left| M \right| + \left| \lambda_2 - \lambda_1 \right|^{-1} \left| v_1 \right|.$$

Since we are assuming that B and C stay positive, from (9) and· (10) we

see that, as $\alpha \to 0^-$, λ_1, λ_2 and $(\lambda_2 - \lambda_1)^{-1}$ remain bounded. Thus, also

c_1 and c_2 remain bounded, and from (24) we see that if K reamins bounded,

then for every $\varepsilon > 0$ there are constants A_0, B_0, that do not depend on α,

such that $\left| v(t) \right| \leq A_0 + B_0 t$ for α in $(-\varepsilon, 0)$. Applying this inequality

it is now easy to see that for any $\varepsilon > 0$, $Q(a, b, \lambda_1, s)$ and

$Q(a, b, \lambda_2, s)$ are bounded, uniformly on α, provided that $-\varepsilon < \alpha < 0$.

Thus, we conclude that there are constants $K_1 = K_1(\varepsilon)$, and $K_2(\varepsilon)$, such that

$$\left| F[P^{(a,b)}](s) \right| \leq K_1 / \left| \lambda_1 - si \right| + K_2 / \left| \lambda_2 - si \right|.$$

This means that the only value for which $F[P^{(a,b)}](s)$ diverges as $\alpha \to 0^-$

is $s = \beta$. Also, there is no obvious reason why $F[P^{(a,b)}](\beta)$ should vanish

as $a \to \infty$ (provided that we keep the difference $b - a$ constant).

3.3.3 Conclusions

In summary, we have shown that $F[v^{(a,b)}](\beta)$ diverges as $\alpha \to 0^-$, that

β is the only value for which this may happen, that for α negative and

constant, but sufficiently close to zero, the graphs of the absolute values

of the real and imaginary parts of $F[v^{(a,b)}](s)$ will have spikes at $s = \beta$,

and that the magnitude of these spikes need not decrease with time (i.e., as

$a \to \infty$).

In [7, p. 784], Day equates the nonlinear natural frequency with the

ratio Q_s/C_s (which, in our notation, equals B/C). Later on, (on p. 786),

he notes that the nonlinear natural frequency is actually not B/C, but a

number close to it. In this paper we have gone one step further and shown

that β (i.e. the transient frequency of the linear part of (5)), and the

nonlinear natural frequency are one and the same. This is a very surprising

result.

On the practical side, our conclusions suggest that, all other things being equal, the introduction of nonlinearities (as induced, e.g. by deadbands) in a mechanical system, may give an earlier warning of the approach to the instability boundary.

4. Examples

We now study the behavior of the solutions of (5) for $C = 240$, $A = 0$, $\delta = 0.0000285$, $K = 1,305,000$, $f(t) = uw^2 \exp(iwt)$, $u = 0.00006915$, and $w = 1,000\pi s$, where s will vary. We also make the realistic assumption -based on empirical data- that the bearing stiffness changes with the forcing frequency w, by setting $B = 60w$. Let f_c (the "critical frequency") be defined to equal $(A+K)^{1/2}/(2\pi) = K^{1/2}/(2\pi)$. We readily see that $f_c \doteq 181.8$ Hz., and that the value of s that corresponds to f_c is $s_c \doteq 1.4545$. For $s = 10/3$ our example reduces to Example 1 of [7].

Let $f_1 = w/2\pi$ denote the forcing frequency; clearly $f_1 = 500$ s. We know that (5) will be stable for $s < s_c$, and unstable for $s > s_c$. In Figs. 2 through 5 we show, for various values of s, plots of the numerical solutions of (5), (obtained by a fourth order Runge-Kutta algorithm), and of PSD's for the real part y and imaginary part z of v. The solution plots are for $0.1 < t < 0.256$, and the PSD plots for the window [0, 0.256]. Note that all the PSD plots have two distinct spikes: one corresponding to the forcing frequency, and one corresponding to the nonlinear natural frequency. For s $= 0.5$ (i.e. far from the stability boundary), the forcing function f(t) dominates the perturbation term P(t). Thus, the solution is nearly circular (we see a thick circular curve; the thickness is caused by P(t)), and the PSD plots exhibit larger spikes for the forcing frequency than for the nonlinear natural frequency. As s increases, the solution becomes annular, and the nonlinear natural frequency begins to dominate. Finally, for $s > s_c$

the solutions begin to diverge. Since the PSD plots are obtained by approximating Fourier transforms by discrete Fourier transforms, (which are intrinsically bounded) they show no obvious qualitative difference when compared with plots for values of s close to, but smaller than, s_c.

Figures 6 and 7 show PSD plots for s = 1.2 and s = 1.3 and various windows. Note that if we compare the PSD plots for $0 < t < 0.256$ (Figs. 3 and 4) and $0.256 < t < 0.512$ (Figs. 6 and 7), we see a large decrease in the height of the spike that corresponds to the nonlinear natural frequency, and a very small decrease when we compare the plots for $0.256 < t < 0.512$ and $1.024 < t < 1.28$, but there is no change in magnitude on subsequent windows. This is due to the disappearance of the transient terms $F[p_1]$ and $F[p_2]$.

References

1. E. Oran Brigham, The Fast Fourier Transform, Prentice Hall, Englewood Cliffs, 1974.

2. R. G. Bartle, The Elements of Rea. Analysis, John Wiley & Sons, New York, 1964.

3. D. W. Childs, The Space Shuttle main engine high-pressure fuel turbopump rotordynamics instability problem, Trans. ASME, J. Engineering for Power, 48-57 (January 1978).

4. D. W. Childs, Rotordynamic characteristics of the HPOTP (high pressure oxygen turbopump) of the SSME (Space Shuttle main engine), NASA MSFC Contract NAS8-34505, Turbomachinery Laboratories Report FD-1-84 (30 January 1984).

5. E. A. Coddington and N. Levinson, Theory of Ordinary Differential Equations, McGraw Hill, 1955. Reprint, Robert E. Krieger Publishing Co., Malabar, Florida, 1984.

6. R. A. Collacott, Vibration Monitoring and Diagnosis, John Wiley & Sons, New York, 1979.

7. W. B. Day, Asymptotic Expansions in Nonlinear Rotordynamics, Quart. Appl. Math. 44 (1987), 779-792.

8. P. K. Gupta, L. W. Winn, and D. B. Wilcock, Vibrational characteristics of ball bearings, Trans. ASME, J. of Lubrication Technology, 99F No. 2 (1977), 284-189.

9. J. K. Hale, Ordinary Differential Equations, 2nd Ed. Robert E. Krieger Publishing Co., Malabar, Florida, 1980.

10. H. H. Jeffcott, The lateral vibration of loaded shafts in the neighborhood of a whirling speed - The effect of want of balance, Philos. Mag., Series 6, 37 (1919), 304-314,

11. B. F. Rowan, Rotordynamics Technical Manual, Rockwell International, Rocketdyne Division, Canoga Park, California, November 1981.

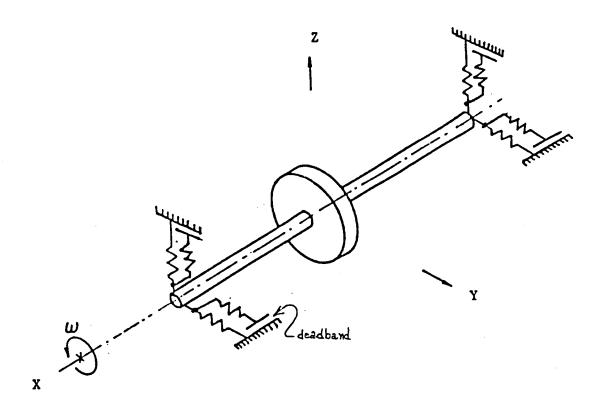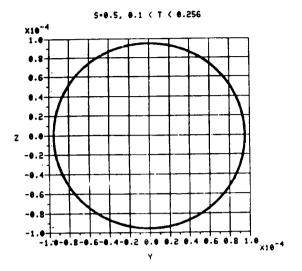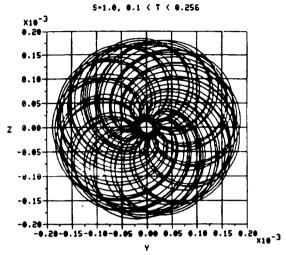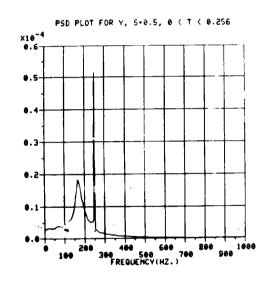12. T. T. Yamamoto, On critical speeds of a shaft, Mem. Fac. Engineering, Nagoya Univ. 6 (1954), 106-174.

FIG. 1

FIG. 2

S=1.1, 0.1 < T < 0.256

S=1.2, 0.1 < T < 0.256

PSD PLOT FOR Y, S=1.1, 0 < T < 0.256

PSD PLOT FOR Y, S=1.2, 0 < T < 0.256

PSD PLOT FOR Z, S=1.1, 0 < T < 0.256

PSD PLOT FOR Z, S=1.2, 0 < T < 0.256

FIG. 3

S=1.3, 0.1 < T < 0.256

S=1.4, 0.1 < T < 0.256

PSD PLOT FOR Y, S=1.3, 0 < T < 0.256

PSD PLOT FOR Y, S=1.4, 0 < T < 0.256

PSD PLOT FOR Z, S=1.3, 0 < T < 0.256

PSD PLOT FOR Z, S=1.4, 0 < T < 0.256

FIG. 4

S=1.5, 0.1 < T < 0.256

S=2.0, 0.1 < T < 0.256

PSD PLOT FOR Y, S=1.5, 0 < T < 0.256

PSD PLOT FOR Y, S=2.0, 0 < T < 0.256

PSD PLOT FOR Z, S=1.5, 0 < T < 0.256

PSD PLOT FOR Z, S=2.0, 0 < T < 0.256

FIG. 5

FIG. 6

FIG. 7